Infrared Spectra of the H_3N-HBr Complex in Solid Ne, Ne/Ar, Ar, Kr, and N_2. Strong Matrix Effects on a Hydrogen-Bonded Complex

Lester Andrews* and Xuefeng Wang

Department of Chemistry, University of Virginia, Charlottesville, Virginia 22904-4319

Received: March 1, 2001; In Final Form: April 18, 2001

Ammonia and hydrogen bromide vapors from the thermal decomposition of NH_4Br were co-deposited with excess neon at 4−5 K to form the H_3N-HBr complex. New 1208.8 and 1079.9 cm^{-1} infrared absorptions are assigned to the H−Br stretching and symmetric NH_3 bending modes of the 1:1 complex. Vibrational assignments are supported by $^{15}NH_4Br$, ND_4Br, $^{15}ND_4Br$, and mixed H, D isotopic substitution. Complementary experiments were done with neon/argon mixtures, argon, krypton, and nitrogen to investigate the 1:1 complex in a range of matrix environments. The above modes are shifted to 729.3 and 1146.7 cm^{-1} in solid argon, owing to an increased interaction with the matrix and the resulting increased proton sharing. The neon matrix spectrum suggests a strong hydrogen bond, slightly stronger than in the gas-phase complex, but not as strong as found in the argon and krypton matrix hosts, owing to increased solvation by the more polarizable matrix atoms and more proton transfer. The strong nitrogen matrix infrared absorption at 1392.2 cm^{-1} shows a 5.2 cm^{-1} ^{15}N shift, 1336.6 and 1134.8 cm^{-1} mixed H, D and 1058.0 cm^{-1} ND_4Br counterparts, and is better described as a mixed N−H stretching, symmetric NH_3 bending mode, which suggests even more proton transfer in the nitrogen host. These and earlier matrix isolation experiments show that the matrix environment markedly affects the hydrogen bonding interaction and the degree of proton transfer in the polar H_3N-HBr complex.

Introduction

The ammonia complexes with HF, HCl, and HBr are unique subjects for the investigation of hydrogen bonding because of their simplicity and the trend in HX ionic dissociation energies, which governs the ease of proton transfer. These complexes have been examined first by quantum chemical calculations,[1−4] followed by matrix infrared spectroscopy,[5−10] and then by microwave spectroscopy in a supersonic jet.[11−13] Although each H_3N-HX complex is characterized as a simple molecular complex in the gas-phase ground vibrational state, there is evidence in the halogen nuclear quadrupole coupling constants for a very small amount of ionic character, which increases from the HCl to the HBr complex.[13] The infrared spectrum necessarily examines the first excited vibrational state, which will be more anharmonic, more ionic, and interact more with a matrix host in the above order. Consistent with that finding, the matrix infrared spectra of H_3N-HF reveal a diagnostic H−F fundamental (3106 and 3041 cm^{-1} in neon and argon, respectively) slightly below the gas-phase value (3220 ± 10 cm^{-1}), but the H_3N-HCl complex exhibits widely differing H−Cl absorptions in solid neon (2084 cm^{-1}) and argon (1371 cm^{-1}), and the gas-phase infrared spectrum has not been recorded.[6,10,14−16] This trend is explained by the stronger interaction of the more polarizable argon matrix with the H_3N-HCl complex, which increases the degree of ionic dissociation, i.e., proton transfer,[16] and is in accord with a recent comparison of matrix infrared and gas-phase microwave observations.[17] In solid argon the H_3N-HBr complex exhibits a very low antisymmetric N−H−Br stretching mode (729 cm^{-1}), which is near the strong antisymmetric stretching mode (728 cm^{-1}) for $(Br-H-Br)^-$; these low frequencies have been logically interpreted as evidence for a significant degree of proton sharing.[8,17,18] The three H_3N-HX complexes have been examined by MP2 calculations and increased anharmonicity in $v = 0$ and $v = 1$ levels and increased interaction with matrix hosts noted for the above order.[19−21]

In view of the clear argon matrix effect on the infrared spectrum of H_3N-HBr, it is desirable to investigate this complex in the more inert neon matrix host. Furthermore, the value of ^{15}N and D substitution for characterizing the vibrational modes has been demonstrated for H_3N-HCl,[16] and neither of the primary works[7,8] on H_3N-HBr employed isotopic substitution. We report here infrared spectra of the H_3N-HBr complex in Ne, Ne/Ar, Ar, Kr, and N_2 matrices, a comparison of hydrogen bonding trends in the H_3N-HX model complexes, and evidence for more proton transfer in the more strongly interacting nitrogen matrix.

Experimental and Computational Section

Ammonia and hydrogen bromide vapors from thermal decomposition of solid NH_4Br were co-deposited with excess neon at 3 mmol/h onto a 5 K (Heliplex APD Cryogenics) CsI window for two or three 30 min periods, and infrared spectra were recorded on a Nicolet 750 instrument at 0.5 cm^{-1} resolution. The solid NH_4Br (Mallinckrodt) was thoroughly degassed and heated[22] by heating tape to 100−130 °C in a Teflon bore right-angle valve (Ace Glass, 3 mm) controlled sample tube with 11 cm sidearm through a vacuum fitting to a point 2 cm from the cold surface (Figure 1). The internal sidearm was heated by resistance wire to approximately 130 °C to prevent the condensation of solid NH_4Br. The NH_3 concentration in the neon matrix is estimated to be about 0.1% from published spectra.[23] Deuterated samples were prepared by exchanging NH_4Br with D_2O in the sample tube three times and evaporating residual D_2O at 40−50 °C, which serves to exchange deuterate

10.1021/jp010812x CCC: $20.00
Published on Web 06/09/2001

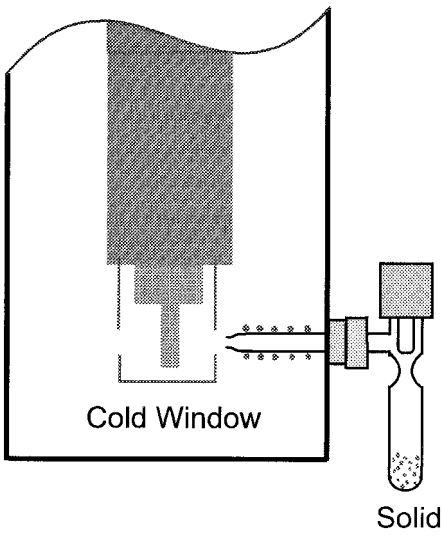

Figure 1. Schematic diagram of Teflon-bore right-angle valve controlled sample tube for thermal decomposition of NH_4Br and co-deposition of NH_3 and HBr with matrix gas. The matrix gas spray-on line is behind and aligned with the internal sidearm.

the sidearm and allow for the delivery of relatively pure DBr and ND_3 into the matrix. Solid $^{15}NH_4Br$ (98% ^{15}N, Aldrich) was used directly, and $^{15}ND_4Br$ was also prepared by exchange with D_2O. A small statistical H, D sample was made by recrystallizing equal parts NH_4Br and ND_4Br from one drop each of H_2O and D_2O in the sample tube. Mixed $^{14}NH_4Br/^{15}NH_4Br$ was prepared by grinding equal parts together with a mortar and pestle, and the remaining sample was recrystallized from excess D_2O three times in the sample tube to prepare mixed $^{14}ND_4Br/^{15}ND_4Br$.

Density functional theory (DFT) calculations[24] were used to predict frequencies for the H_3N-HCl and H_3N-HF complexes.[16] The B3LYP and BPW91 functionals, 6-311+G** basis sets and LANL2DZ pseudopotential[25−28] were employed here for the H_3N-HBr complex. All geometrical parameters were fully optimized, and harmonic vibrational frequencies were computed analytically at the optimized structures.

Results

Neon. Infrared spectra are shown in Figure 2 for 30 and 60 min deposition periods and subsequent annealings to 8, 10, 11 and 13 K. The spectra of NH_3, $(NH_3)_2$, HBr, $(HBr)_2$, and $(HBr)_3$ are in agreement with previous reports based on reasonable argon−neon matrix shifts;[23,29,30] note that the HBr and NH_3 monomer species dominate in each spectral region, but the population of dimer species increases with sample thickness. The dominance of HBr monomer is even more striking when the substantially increased infrared intensity of $(HBr)_2$ is considered. The strongest new feature at 1079.9 cm^{-1} is associated with weaker 1208.8 and 3444.8 cm^{-1} absorptions. Table 1 lists all of the observed bands. Annealing to 8 and 11 K had little effect on the above new bands, but a sharp 1120.4 cm^{-1} band increased markedly, and 1389.2, 1411.6, 1454.6, and 1485.3 cm^{-1} bands increased. Diffusion on annealing cycles

TABLE 1: Infrared Absorptions (cm^{-1}) from Co-deposition of Ammonia and Hydrogen Bromide Vapor from Ammonium Bromide with Excess Neon at 5 K

NH_4Br	$^{15}NH_4Br$	ND_4Br	$^{15}ND_4Br$	identification
3465.7	3455.4	2573.5	2561.4	NH_3, ν_3 site
3444.8	3435.7	2569.3	2556.6	H_3N-HBr
3412.6	3404.4	2541.0	2529.6	$(NH_3)_2$, "ν_3"
3364.3	3361.4	2420.7	2415.6	NH_3, ν_1
3319.8	3314.9			$(NH_3)_2$, "ν_1"
3122[a]	3115	2328	2322	NH_4Br, ν_3
3043[a]	3034	2248	2242	NH_4Br
2568.2	2568.2	1842.4	1842.4	HBr, R(0)
2557.4	2557.4	1838.5	1838.5	HBr site
2520.5	2520.5	1809.5	1809.5	$(HBr)_2$
2487.4	2487.4	1787.3	1787.3	$(HBr)_3$
2463.2	2463.2	1769.5	1769.5	$(HBr)_x$
2416.0	2416.0	1740.7	1740.7	H_2O-HBr
1817.3	1811.2			$(NH_3)(HBr)_2$
1732.6[b]	1726.5			$(NH_3)_x(NBr)_y$
1728	1722	1308	1303	NH_4Br
1644.8	1641.4	1199.9	1196.3	NH_3, ν_4
1486	1480	1153.4	1149.9	$(NH_3)_x(NBr)_y$
1454.6	1448.5	1121.5	1115.6	$(NH_3)_x(NBr)_y$
1439[a]	1431	1087	1082	NH_4Br
1428	1421			$(NH_3)_x(NBr)_y$
1411.6[b]	1405.7	1103.6	1096.7	$(NH_3)_x(NBr)_y$
1409.4[a]	1403.1	1067	1062	$(NH_3)_x(NBr)_y$
1389.2	1383.0	1069.8	1062.9	$(NH_3)_x(HBr)_y$
1208.8	1202.4	947.9	945.8	H_3N-HBr
1120.4	1115.3	865.8	858.6	$(H_3N)(HBr)_2$
1115.5	1110.3	863.0	855.7	$(H_3N)(HBr)_2$
1079.9	1074.5	831.7	824.4	H_3N-HBr
1031.6	1026.5	802.3	796.1	NH_3-H_2O
1019.4	1014.7	793.1	786.3	$(NH_3)_3$
994.0	989.4	779.6	773.1	$(NH_3)_2$
968.2	964.1	767.4	761.0	NH_3, ν_2
960.7	956.6	757.0	750.6	NH_3, ν_2 site
811	811	570	570	$(HN_3)(HBr)_2$
761	761	537	537	$(NH_3)_x(HBr)_y$

[a] Features observed on final annealing: bands also observed at nearly the same wavenumber on window background with no matrix. [b] Sharp band.

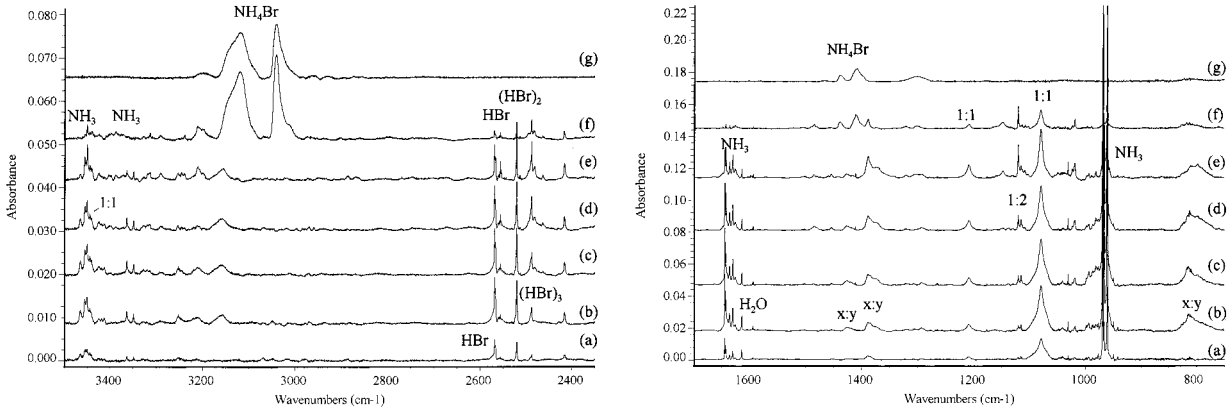

Figure 2. Infrared spectra in the 3500−2350 and 1700−750 cm^{-1} regions for NH_4Br vapors co-deposited with excess neon at 4−5 K: (a) after sample deposition for 30 min, (b) after sample deposition for 60 min, (c) after annealing to 8 K, (d) after annealing to 10 K, (e) after annealing to 11 K, (f) after annealing to 13 K, and (g) after annealing to 70 K leaving only solid NH_4Br.

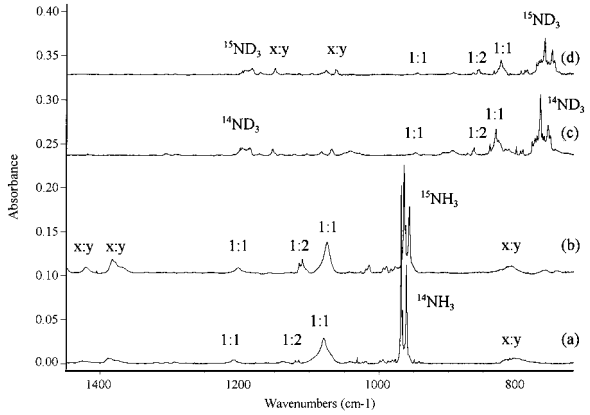

Figure 3. Infrared spectra in the 1460−720 cm^{-1} region for isotopic ammonium bromide vapors co-deposited with excess neon at 4−5 K for 60 min. (a) NH_4Br, (b) $^{15}NH_4Br$, (c) ND_4Br, and (d) $^{15}ND_4Br$.

decreased the NH_3 and HBr monomers and increased $(NH_3)_2$, $(HBr)_2$, and $(HBr)_3$, and also increased the broad 811 cm^{-1} band.

The above absorptions shifted in similar experiments using isotopic ammonium bromide samples as shown in Figure 3. With $^{15}NH_4Br$, the first new product appeared at 1074.5 and 1202.4, and 3435.7 cm^{-1} and 1115.3, 1383.0, 1405.7, 1448.5, and 1479.5 cm^{-1} counterpart bands increased on annealing. A mixed $^{14}NH_4Br/^{15}NH_4Br$ sample gave partially resolved doublets for the first new features, sharp resolved doublets for the 1120.4 and 1454.6 cm^{-1} bands and a 1411.5, 1408.1, 1405.7 cm^{-1} triplet. With relatively pure isotopic ND_4Br (note the weak sharp NHD_2 band at 840.4 cm^{-1}) the primary bands were found at 831.7, 947.9, and 2569.3 cm^{-1} and the 865.8, 1068.4, and 1153.4 cm^{-1} bands increased on annealing. With $^{15}ND_4Br$ the first new product was observed at 825.4, 945.8, and 2556.6 cm^{-1}, and the 858.4, 1062.8, and 1150.4 cm^{-1} bands increased on annealing. Two mixed $^{14}ND_4Br/^{15}ND_4Br$ experiments gave sharp resolved 2569.4, 2556.7 cm^{-1} and 831.7, 824.4 cm^{-1} doublets and a 947 cm^{-1} band for the first product, a sharp 865.8, 858.6 cm^{-1} doublet, and a 1153.4, 1151.3, 1149.9 cm^{-1} triplet for annealing products. One experiment with the statistical H, D sample gave strong 1080, 1018, and 934 cm^{-1} bands in proportion to the ammonia precursors (the 832 cm^{-1} band was masked by NHD_2); the weaker 1209 and 948 cm^{-1} features were observed without intermediate components. Several experiments were done for each isotopic sample with different sample-tube temperatures: increasing the sample temperature favored the bands that increased on annealing relative to the first product bands. In particular, the broad 811 cm^{-1} band was favored at higher sample evaporation temperature.

Argon. A set of isotopic ammonium bromide experiments was done with argon condensed at 8 K. The HBr monomer band at 2568.3 cm^{-1} and site splitting at 2558.2 cm^{-1} dominated the region; the $(HBr)_2$ band at 2496.3 cm^{-1} was much weaker (0.2×), and the $(HBr)_3$ absorption[30] at 2464.7 cm^{-1} was not observed. Figure 4 illustrates spectra for the natural isotopic sample in the 1800−500 cm^{-1} region: note the sharp 999.9 cm^{-1} $(NH_3)_2$ band with 5% of the absorbance of the NH_3 band at 974.6 cm^{-1}. The primary product absorptions at 3420.8, 1146.7, 729.3, and 591.3 cm^{-1} (labeled 1:1) are in excellent agreement with bands observed by Barnes and Wright[8] and assigned to H_3N-HBr. Annealing to 20 and 30 K increases these bands to double their initial absorbance, but weaker bands at 1731.9, 1526.7, 1426.0, 1397.9, 1200.4, and 1111.2 cm^{-1} increase a larger proportion and increase further on 35 K annealing while the primary product bands decrease slightly. There is also slight growth in $(HBr)_2$ and $(NH_3)_2$ on annealing.

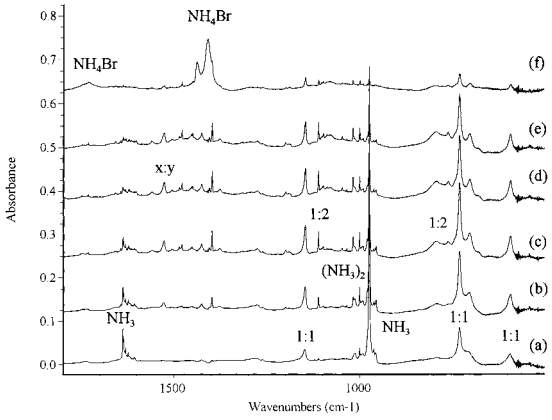

Figure 4. Infrared spectra in the 1800−500 cm^{-1} region for NH_4Br vapors co-deposited with excess argon at 8−9 K: (a) after sample deposition for 60 min, (b) after annealing to 20 K, (c) after annealing to 30 K, (d) after annealing to 35 K, (e) after annealing to 40 K, and (f) after annealing to 45 K.

TABLE 2: Infrared Absorptions (cm^{-1}) from Co-deposition of Ammonia and Hydrogen Bromide Vapor from Ammonium Bromide with Excess Argon at 8−9 K

NH_4Br	$^{15}NH_4Br$	ND_4Br	$^{15}ND_4Br$	identification
3447.0	3439.0	2556	2544	NH_3, ν_3
3420.8	3412.1	2548.0	2535.2	H_3N-HBr
3400.3	3392.1	2527.2	2515.3	$(NH_3)_2$, "ν_3"
3344.8	3342.0	2413.3	2409.1	NH_3, ν_1
3310.3	3306.4			$(NH_3)_2$, "ν_1"
2568.3	2568.3	1844.6	1844.6	HBr, R(0)
2501		1925	1915	$(NH_3)_x(HBr)_y$
2558.2	2558.2	1837.6	1837.6	HBr site
2496.3	2496.3	1792.4	1792.4	$(HBr)_2$
2464.7	2464.7	1771.1	1771.1	$(HBr)_3$
2426.5	2426.5	1744.6	1744.6	$(HBr)_x$
2396	2396	1728	1728	H_2O-HBr
1823	1817	1330.3	1324.1	$(NH_3)(HBr)_2$
1731.9[a]	1725.8			$(NH_3)_x(HBr)_y$
1638.5	1635.3	1190.8	1187.2	NH_3, ν_4
1526.7	1521.3	1152.7	1148.5	$(NH_3)_x(HBr)_y$
1479.3	1473.5	1128.4	1121.8	$(NH_3)_x(HBr)_y$
1426.0	1419.6	1083.3	1076.3	$(NH_3)_x(HBr)_y$
1397.9[a]	1391.8	1071.5	1064.7	$(NH_3)_x(HBr)_y$
1276.3	1268.3			$(NH_3)_x(HBr)_y$
1200.4	1197.8			$(NH_3)_x(HBr)_y$
1146.7	1142.4	906.6	899.8	H_3N-HBr
1111.2	1105.8	858.1	850.8	$(H_3N)(HBr)_2$
1035.0	1029.9	805.1	798.1	H_3N-H_2O
1018.0	1013.4	791.7	785.3	$(NH_3)_3$
999.9	995.3	780.4	773.9	$(NH_3)_2$
974.6	970.5	759.7	752.9	NH_3, ν_2
		700.3	696.6	D_3N-HBr
795	794	533	533	$(H_3N)(HBr)_2$
729.3	725.5	480.8	479.2	H_3N-HBr
702.0	699.7			H_3N-HBr site
591.3	588.6			H_3N-HBr

[a] Sharp band.

A 40 K annealing decreases the primary bands more than the second set. The final annealing to 45 K leaves little (about 20% of maximum intensity) of the above band and produces strong new ammonium bromide absorptions at 3121, 3042 (not shown), 1440, and 1410 cm^{-1} in solid argon. After the matrix experiment, the room-temperature window reveals broad 3130, 3041, 1751, and 1405 cm^{-1} bands appropriate for solid ammonium bromide.[31]

The above absorptions shifted with $^{15}NH_4Br$, ND_4Br, and $^{15}ND_4Br$ substitution as listed in Table 2 and illustrated in Figure 5. Two experiments with mixed $^{14}NH_4Br/^{15}NH_4Br$ samples gave resolved pure isotopic doublets for the upper two and partially

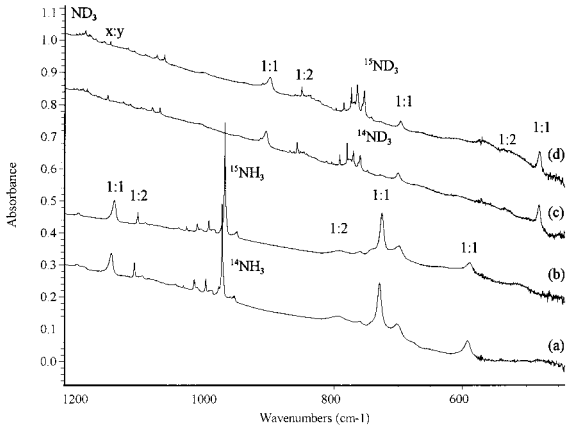

Figure 5. Infrared spectra in the 1220−440 cm^{-1} region for isotopic ammonium bromide vapors co-deposited with excess argon at 8−9 K for 60 min after annealing to 30 K. (a) NH_4Br, (b) $^{15}NH_4Br$, (c) ND_4Br, and (d) $^{15}ND_4Br$.

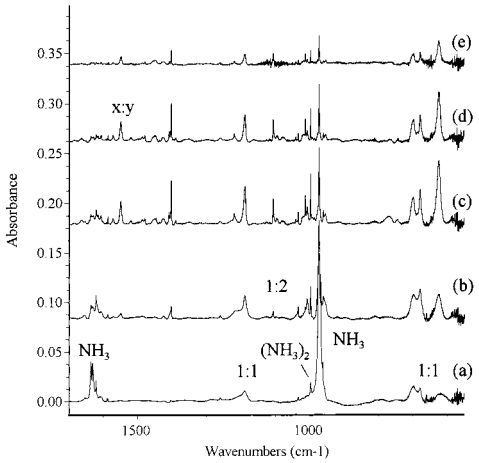

Figure 6. Infrared spectra in the 1700−550 cm^{-1} region for NH_4Br vapors co-deposited with krypton containing 10% neon at 5 K: (a) after sample deposition for 60 min, (b) after annealing to 20 K, (c) after annealing to 30 K, (d) after annealing to 35 K, and (e) after annealing to 40 K.

resolved doublets for the lower two primary product absorptions; sharp isotopic doublets were observed for the 1111.2 and 1397.9 cm^{-1} bands, broad doublets for the 1479.3 and 1526.7 cm^{-1} absorptions, and a triplet was found for the 1426.0 cm^{-1} feature. Similar investigations with $^{14}ND_4Br/^{15}ND_4Br$ produced doublets at 2548.1, 2535.3 cm^{-1}, 906.0, 899.2 cm^{-1}, and a 480 cm^{-1} band for the primary product, and sharp pure isotopic doublets at 858.1, 850.8 cm^{-1}, 1071.5, 1064.8 cm^{-1}, and 1083.3, 1076.3 cm^{-1}. One experiment with the statistical H, D sample gave the 1146.7 cm^{-1} band, a sharp 1109.1 cm^{-1} peak, broad 1079 and 980 cm^{-1} absorptions, a broad band with peaks at 729.3, 720.2, 710.8, and 701.3 cm^{-1}, and a broad 595 cm^{-1} feature.

Neon/Argon. Experiments were performed with 2, 5, 10, and 20% argon in neon. With 2% Ar in Ne, bands were observed at 1388, 1209, 1080.6, and 811 cm^{-1}. Annealing to 6, 8, 10, and 12 K broadened and decreased these bands while a new broad 780 cm^{-1} band appeared: the 1388 cm^{-1} band shifted stepwise to 1396 cm^{-1} and the 1080.6 cm^{-1} shifted stepwise to 1084.3 cm^{-1}. Similar results were obtained with the $^{15}NH_4Br$ counterparts. With 5% Ar in Ne, 1392, 1081, and 1209 cm^{-1} bands were observed on deposition: annealing to 6 K shifted the former to 1398 cm^{-1}, decreased the latter two bands and a broad 766 cm^{-1} band appeared. Further annealing shifted the former stepwise to 1400 cm^{-1}, destroyed the latter two bands, increased the 766 cm^{-1} feature, and produced a weak 1160 cm^{-1} absorption. With 10% Ar in Ne, 1403, 1160, 1113, and 736 bands were observed, and with 20% Ar in Ne, 1399.4, 1149.8, 1111.4, and 732 cm^{-1} bands were observed: the 1210 ± 10 and 1080 ± 10 cm^{-1} regions were bare.

Krypton. Ammonium bromide experiments were done in krypton with 10% neon on a 5 K substrate. Diffusion and association of NH_3 and HBr and loss of Ne take place on annealing. The spectra in Figure 6 reveal weak bands at 1188.6, 700.3, and 624.5 cm^{-1} on deposition that increase on annealing to 20 K and reach maximum intensity on annealing to 30 K. Additional bands at 1549.9, 1402.6, and 1107.0 cm^{-1} are extremely weak on deposition, increase markedly on 20 K annealing, and also reach maximum intensity on 30 K annealing. Ammonia and HBr clusters also increase on annealing: note that the $(NH_3)_2$ absorbance at 998.3 cm^{-1} on deposition is a few percent of the NH_3 band at 974.0 cm^{-1}; the same relationship is found for $(HBr)_2$ and HBr.

A complete set of isotopic experiments in solid krypton gave the absorptions listed in Table 3. Unfortunately, the deuterium counterparts of the 700.3 and 624.5 cm^{-1} bands shifted below the instrumental limit (430 cm^{-1}). A mixed $^{14}NH_4Br/^{15}NH_4Br$ experiment gave an unresolved doublet for the 1188.6 cm^{-1} band, resolved pure isotopic doublets for the 1107.0 and 1402.6 cm^{-1} absorptions, and a broad 1549, 1547 cm^{-1} doublet.

TABLE 3: Infrared Absorptions (cm^{-1}) from Co-deposition of Ammonia and Hydrogen Bromide Vapor with Excess Krypton Containing 10% Neon at 5 K[a]

NH_4Br	$^{15}NH_4Br$	ND_4Br	$^{15}ND_4Br$	identification
3434	3426	2551	2539	NH_3, ν_3
3406	3397	2537	2525	H_3N-HBr
3335	3332			NH_3, ν_1
2551.4	2551.4	1833.0	1833.0	HBr
2541.1	2541.1	1826.5	1826.5	HBr site
2491.3	2491.3	1788.8	1788.8	$(HBr)_2$
2467.5	2467.4	1772.6	1772.6	$(HBr)_3$
2437.3	2436.4	1751.2	1751.2	$(HBr)_x$
2389	2389	1723	1723	H_2O-HBr
1636	1633	1189	1185	NH_3, ν_4
1549.9	1546.8			$(NH_3)_x(HBr)_y$
1479.7	1473.7	1128.4	1123.3	$(NH_3)_x(HBr)_y$
1402.6[b]	1396.7	1072.7	1065.8	$(NH_3)_x(HBr)_y$
1188.6[b]	1185.4	947.1	938.5	H_3N-HBr
1107.0[b]	1101.5	842.3	836.2	$(NH_3)(HBr)_2$
1034.6	1029.3	804.0	797.7	H_3N-H_2O
1013.7	1009.0	788.8	782.4	$(NH_3)_3$
998.3	993.7	779.6	772.9	$(NH_3)_2$
974.0	969.8	759.3	752.5	NH_3, ν_2
700.3[b]	691.3	*a*	*a*	H_3N-HBr
678.7[b]	678.3	*a*	*a*	H_3N-HBr
624.5[b]	624.3	*a*	*a*	H_3N-HBr

[a] Not observed, which places deuterium counterparts for the 700−624 cm^{-1} bands below 430 cm^{-1}. [b] The 1402.6, 1188.6, 1107.0, and 700.3 cm^{-1} bands and isotopic counterparts are reported after 30 K annealing to remove neon and allow diffusion.

Nitrogen. Since the H_3N-HBr complex was first characterized in solid nitrogen,[7] a series of nitrogen matrix experiments was performed here using stepwise lower reagent concentrations and a colder 5 K substrate. At this low condensation temperature, the NH_3 and HBr vapor was trapped as monomers (Figure 7) in the lowest reagent concentration (<0.1%) experiment. The very weak 1392 cm^{-1} band observed on sample deposition is the same band assigned to H_3N-HBr by three groups.[7−9] Annealing to 25 K increases a 3402.8 cm^{-1} band and produces structure at 1392.2, 1384.0, and 1372.6 cm^{-1}, a weaker 1211.7 cm^{-1} band (labeled 1:1), absorptions for $(HBr)_2$ and $(NH_3)_2$, and other absorptions near 1750, 1429, 1127, and 795 cm^{-1}

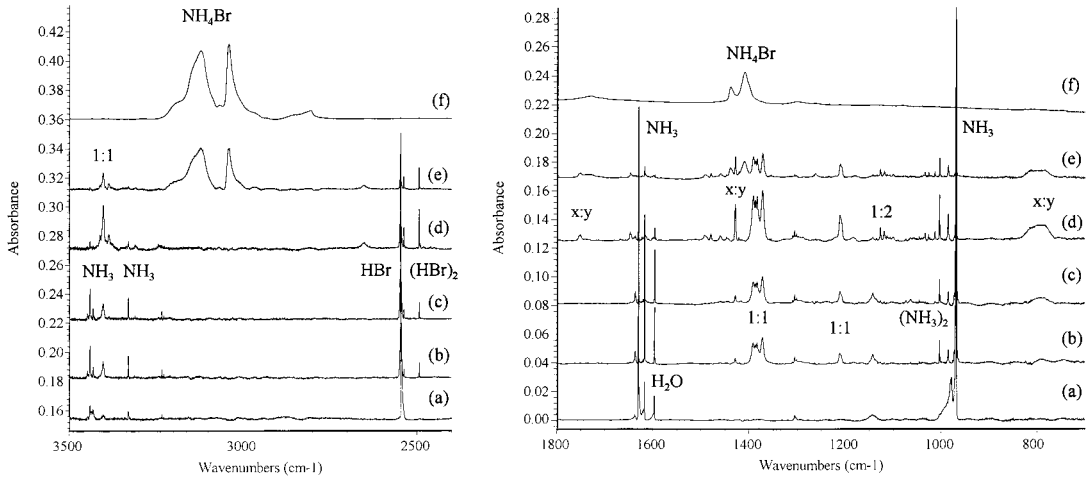

Figure 7. Infrared spectra in the 3500−2350 and 1800−700 cm^{-1} regions for NH_4Br vapors co-deposited with excess nitrogen at 5 K: (a) after sample deposition for 60 min, (b) after annealing to 25 K, (c) after annealing to 32 K, (d) after annealing to 36 K, (e) after annealing to 38 K, and (f) after annealing to 40 K leaving only solid NH_4Br.

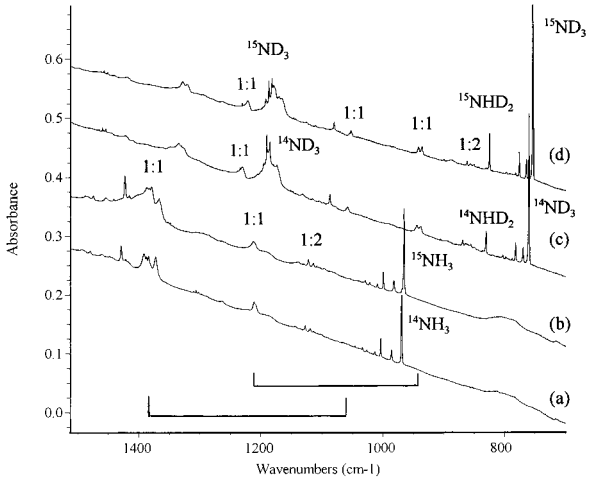

Figure 8. Infrared spectra in the 1520−700 cm^{-1} region for isotopic ammonium bromide vapors co-deposited with excess nitrogen at 5 K for 60 min and after annealing to 36 K. (a) NH_4Br, (b) $^{15}NH_4Br$, (c) ND_4Br, and (d) $^{15}ND_4Br$. Bars connect pure isotopic 1:1 complex absorptions.

TABLE 4: Infrared Absorptions (cm^{-1}) from Co-deposition of Ammonia and Hydrogen Bromide Vapor from Ammonium Bromide with Excess Nitrogen at 5 K

NH_4Br	$^{15}NH_4Br$	ND_4Br	$^{15}ND_4Br$	identification
3440.7	3432.5	2557.9	2543.9	NH_3, ν_3
3402.8	3393.9	2536.5	2523.8	H_3N-HBr
3330.4	3327.6	2415.5	2411.6	NH_3, ν_1
3311.8	3307.7	2368.6	2361.4	$(NH_3)_2$, "ν_1"
2545.6	2545.6	1828.9	1828.9	HBr
2537.2	2537.2	1823.1	1823.1	$(HBr)_2$
2493.0	2493.0	1790.5	1790.5	$(HBr)_2$
		1459.8	1457.0	NHD_2
		1335.2	1328.2	$(ND_3)_x(DBr)_y$
1751.0[a]	1744.8			$(NH_3)_x(HBr)_y$
		1234.5	1230.8	NHD_2
		1232	1222	D_3N-DBr
1630.6	1627.5	1190.4	1186.8	NH_3, ν_4
1429.3[a]	1423.2	1087.1	1080.1	$(NH_3)_x(HBr)_y$
1392.2	1387.0	1057.8	1052.5	H_3N-HBr
1384.0	1379.2	1055.5	1050.2	H_3N-HBr site
1372.6	1366.8	1055.2	1050.2	H_3N-HBr site
1211.7	1211.0	943.6	940.6	H_3N-HBr
1208.6		937.7	934.9	H_3N-HBr site
		829.8	824.2	NHD_2
1127.4	1122.1	868.4	861.2	$(H_3N)(HBr)_2$
1119.2	1114.0			$(H_3N)(HBr)_2$
1003.4	998.9	781.8	775.2	$(NH_3)_2$
985.5	981.3	769.5	763.5	$(NH_3)_2$
969.6	965.2	759.3	752.9	NH_3, ν_2
795	795			$(NH_3)_x(HBr)_y$

[a] Sharp band.

also observed previously.[7−9] It is clear from the annealing cycles that the latter absorptions are due to higher order complexes. Final 38 K annealing decreases the 3402, 1392, and 1212 cm^{-1} features most and produces strong 3130, 3041, 1439, and 1405 cm^{-1} bands due to large enough clusters to approximate solid NH_4Br as these bands shift only slightly when all matrix gas is evaporated. The ν_3 and ν_4 fundamentals of solid NH_4Br recorded here at 5 K (Table 1) agree with earlier solid values[31] within 2 cm^{-1}.

Experiments with $^{15}NH_4Br$, ND_4Br, and $^{15}ND_4Br$ using different evaporation temperatures produced isotopic counterparts that were tracked by concentration and annealing behaviors. Figure 8 contrasts isotopic spectra for the important 1500−900 cm^{-1} region recorded after 36 K annealing, and Table 4 lists the band positions. An experiment with the $^{14}ND_4Br$/$^{15}ND_4Br$ sample gave 1/1 doublets for the 2536.5, 1057.8, 943.6 cm^{-1} bands and sites, which were a superposition of the pure isotopic bands. Similar doublets were observed for the sharp 1087.1 and 868.4 cm^{-1} absorptions. Three experiments were done with the statistical H, D sample to find the best conditions for observing mixed H, D isotopic species. The more dilute sample contained NH_3 (969.3 cm^{-1}, 0.043 au), NH_2D (904.3 cm^{-1}, 0.131 au), NHD_2 (829.6 cm^{-1}, 0.120 au), and ND_3 (759.0 cm^{-1}, 0.038 au) bands, HBr (2545.6 cm^{-1}, 0.12 au), and DBr (1828.9 cm^{-1}, 0.04 au) on 5 K sample deposition, and no precursor dimers were observed. Annealing sharpened the precursor peaks and produced precursor dimers, new absorptions (1:1) at 1392.2, 1372.5, 1336.6, 1321.9, 1134.8, 1123.9 cm^{-1} and at 1211.7, (1128.2), 1021.5, 943.6 cm^{-1}, and sharp (1:2) bands at 1036.8, 953.4, 868.2 cm^{-1}. These new absorptions decreased slightly on final 38 K annealing. In addition, the upper region revealed counterparts for the strong 3402.8 cm^{-1} band at 3400.4, 3368.8, 3339.7, 2547.5, and 2537.2 cm^{-1}.

Calculations. DFT calculations were done for the hydrogen-bonded H_3N-HBr structure in C_{3v} symmetry using the B3LYP and BPW91 functionals. The calculated N−Br distances, 3.251 and 3.139 Å, respectively, are near the 3.255 Å microwave value.[11] Clearly the BPW91 functional predicts a stronger

TABLE 5: Frequencies (cm^{-1}), Intensities (km/mol), and Bond Lengths (Å) Calculated for H_3N-HBr Complexes in C_{3v} Symmetry Using Density Functional Theory[a]

BPW91	$H_3N-H-Br$ ($\mu = 6.0$ D), ∠ HN−H: 110.8°
H−N: 1.022	3521 (e, 26), 3403 (a_1, 1), 1616 (e, 25), 1367 (a_1 2879)
N−H: 1.571	1110 (a_1, 1), 933 (e, 54), 287 (e, 12), 175 (a_1, 114)
H−Br: 1.568	
B3LYP	$H_3N-H-Br$ ($\mu = 5.1$ D),[b,c,d] ∠ HN−H: 110.9°
H−N: 1.016	3594.7 (e, 20), 3472.5 (a_1, 1), 1815.7 (a_1, 2009), 1657.7 (e, 26)
N−H: 1.749	1119.0 (a_1, 103), 778.8 (e, 67), 251.8 (e, 14), 154.3 (a_1, 42)
H−Br: 1.502	
B3LYP	$H_3N-H-Br$ (μ= 9.9 D),[e] ∠ HN−H: 109.8°
H−N: 1.0196	3557 (84), 3554 (89), 3442 (17), 1783 (75), 1765 (86),
N−H: 1.168	1460 (3490, 1405 (41), 1400 (47), 1256 (802), 352 (6),
H−Br: 1.860	328 (157), 240 (11)
B3LYP	$H_3N-Br-H$ ($\mu = 0.7$ D),[b] ∠ HN−H: 110.9°
N−H: 1.015	3607 (e, 5), 3480 (a_1, 2), 2513 (a_1, 16), 1666 (e, 26)
N−H: 3.335	1004 (a_1, 202), 264 (e, 2), 65 (a_1, 1) 45 (e, 87)
Br−H: 1.441	
B3LYP	BrH_3NH ($\mu = 9.9$ D),[b] ∠ HN−H: 115.8°
Br−H: 2.624	3436 (a_1, 8), 3336 (e, 74), 3288 (a_1, 291), 1633 (e, 15)
H−N: 1.032	1457 (a_1, 420), 1370 (e, 138), 283 (a_1, 59), 325i (e, 3)
N−H: 1.026	

[a] The 6-311+G** basis and LANL2DZ pseudopotential were used for all calculations; frequencies are followed by (mode symmetry, intensity). [b] Relative energies 0.0, 8.5 and 13 kcal/mol, respectively, for these three isomer structures. [c] Isotopic frequencies for $^{15}NH_4Br$ in order: 3584.8, 3470.4, 1815.7, 1654.5, 1112.7, 777.4, 251.4, 150.8 cm^{-1}; isotopic frequencies for ND_4Br in order: 2646.9, 2479.4, 1295.3, 1202.9, 855.4, 561.7, 181.5, 143.1 cm^{-1}. [d] The 6-311++G** basis produced 1−5 cm^{-1} higher frequencies and 1.739 and 1.503 Å bond lengths. [e] SCI−PCM in heptane solution, SCRF = Dipole.

hydrogen bonding interaction than the B3LYP functional, and both are crude approximations but of value for vibrational frequency trends. Two other structures, the reverse complex H_3N-BrH and BrH_3NH, are given in order of increasing energy at the B3LYP level. Table 5 lists the computed structural parameters and frequencies. The latter has a large dipole moment (9.9D), is 12.0 kcal/mol higher in energy than the hydrogen-bonded complex, and approximates an ammonium cation−bromide anion complex, but the low imaginary frequency indicates that it wants to deform back to H_3N-HBr.

A calculation was done using the self-consistent isodensity polarized continuum model (SCI−PCM)[32] for H_3N-HBr solvated by heptane as an attempt to simulate matrix effects. The solvent option in the Gaussian 98 program offers heptane as the lowest dielectric constant available (1.92), which is slightly higher than that of argon (1.63). This calculation is straightforward using the self-consistent reaction field (SCRF) set to Dipole for geometry optimization and frequencies; the results are included in Table 5.

Finally, hydrogen bromide and $(HBr)_2$ were computed at the B3LYP level. The calculated HBr frequency 2547 cm^{-1} (1 km/mol) and bond length (1.437 Å) are excellent approximations to the gas-phase values (2559 cm^{-1} anharmonic observed value, 1.414 Å).[32] The calculated dimer bond lengths 1.437, 2.821, and 1.442 Å and stretching frequencies are 2547 cm^{-1} (4 km/mol) and 2491 cm^{-1} (112 km/mol) show the effects of hydrogen bonding. Deuterium substitution gives 1813 cm^{-1} (0.5 km/mol) for DBr and 1813 cm^{-1} (2 km/mol) and 1773 cm^{-1} (56 km/mol) for $(DBr)_2$.

Discussion

The ammonia−hydrogen bromide complexes in different matrix environments will be identified on the basis of isotopic substitution and proportional growth on sample annealing, and bonding trends in matrix hosts will be considered.

Argon. Identification of the H_3N-HBr complex in solid argon is straightforward. The natural isotopic reagent gases were co-deposited in excess argon, and 3420, 1398, 1148, 1112, 729, and 591 cm^{-1} absorptions were assigned to the 1:1 complex.[8] The primary product absorptions at 3420.8, 1146.7, 729.3, 591.3 cm^{-1} observed here with much lower reagent concentrations and argon deposition at 8 K increase 2-fold on annealing to 20 and 30 K, but much weaker 1731.9, 1526.7, 1397.9, 1200.4, and 1111.2 cm^{-1} bands increase 10-fold, and annealing to 35 K slightly *increases* the latter bands and *decreases* the former absorptions (Figure 4). The latter bands are clearly due to higher order complexes. Final annealing to 45 K reduces all of the above bands and produces strong characteristic NH_4Br absorptions.

The sharp 1111.2 cm^{-1} band exhibits a 5.4 cm^{-1} ^{15}N shift, and the ND_3 counterpart at 858.1 cm^{-1} exhibits a 7.3 cm^{-1} ^{15}N shift, all characteristic of a symmetric NH_3 bending mode. Both bands gave sharp, pure isotopic doublets in mixed $^{14/15}N$ experiments, indicating the vibration of a single NH_3 unit. The 1111.2 cm^{-1} band is assigned to the 1:2 complex $(NH_3)(HBr)_2$ blue shifted from the 974.6 cm^{-1} ammonia value. Weak 1823 and broad 795 cm^{-1} bands also associated with this species are probably due to N−H and Br−H−Br antisymmetric stretching modes, respectively. Recall that $(Br-H-Br)^-$ absorbs at 728 cm^{-1}.[18] The $(HBr)_2$ dimer also increases on annealing, but measuring the HBr monomer/$(HBr)_2$ dimer population in these experiments depends critically on the relative mode intensities: our DFT calculations suggest that $(HBr)_2$ is a 100-fold stronger absorber than HBr. Hence, the overwhelming majority of the HBr reagent is trapped as the monomer in these experiments.

The sharp 1397.9 cm^{-1} band is in the ν_4 ammonium ion region, but no counterpart absorption appears in the 3100 cm^{-1} ν_3 region. The sharp weaker 1731.9 cm^{-1} absorption tracks with the stronger 1397.9 cm^{-1} band and is in the $\nu_4+\nu_6$ region for NH_4Br.[31] Note that these absorptions exhibit the same 6.1 cm^{-1} ^{15}N shift, so the lower frequency interval involves no nitrogen motion if this is a combination band. The annealing behavior in Figure 4 shows that the 1731.9 and 1397.9 cm^{-1} bands are due to a higher order complex related to but smaller than the solid material. Since DFT calculations have suggested that proton transfer occurs in the 2:2 $(NH_3)_2(HCl)_2$ complex,[34] it is reasonable to expect higher complexes to be ionic and like the solid. The torsional fundamental deduced here for this small ionic cluster (1731.9 − 1397.9 = 334.0 cm^{-1}) is in excellent agreement with the solid NH_4Br value (319 or 335 cm^{-1}).[31] Several higher order cluster absorptions in these regions are simply identified as *x*:*y*, since we cannot determine their stiochiometry. Finally, solid NH_4Br is the ultimate annealing product (Figure 4f).

More information about the 3420.8, 1146.7, 729.3, and 591.3 cm^{-1} absorptions assigned to H_3N-HBr can be obtained from the new isotopic data reported here (Figure 5). First, these bands appear as pure isotopic or partially resolved doublets in mixed $^{14}NH_4Br/^{15}NH_4Br$ experiments, which verifies the participation of a single NH_3 molecule. The 3420.8 cm^{-1} band shows a −8.7 cm^{-1} ^{15}N shift and is appropriate for the NH_3 (e) stretching mode in the complex. The 1146.7 cm^{-1} band must be assigned to the symmetric $^{14}NH_3$ (a_1) bending mode based on the isotopic shifts with $^{15}NH_3$ (−4.3 cm^{-1}), ND_3 (−240.1 cm^{-1}), and

TABLE 6: Frequencies (cm^{-1}) Assigned to Ammonia, HCl, and HBr Complexes in Solid Matrices

	H−X str	sym NH_3 bend	H−X bend	antisym NH_3 str
H_3N−HCl in Ne[a]	2084	1060	709	
Ar[a,b]	1371	1070	734	3430
Kr[a]	1218	1072	737	3420
N_2[a,b,c]	702	1251	628?	3420
H_3N−HBr in Ne	1209	1080		3445
Ar[d]	729	1146	591	3421
Kr	700	1188	624	3407
N_2	1392[e]	1212[e]		3403

[a] Reference 16. [b] Reference 6. [c] Reference 5. [d] Reference 8 and this work. [e] The 1392 cm^{-1} band is reassigned to the predominately N−H stretching mode and the 1212 cm^{-1} band to the largely symmetric ammonia bending mode in the H_3N−H−Br complex; these two a_1 modes are mixed coordinates. The much weaker N−H−Br bending mode is not observed.

$^{15}ND_3$ (−246.9 cm^{-1}). The H/D ratio (1.265) is just below that for ammonia (1.283) and the 14/15 ratio (1.0037) is likewise with respect to ammonia (1.0042). The slightly stronger 729.3 cm^{-1} absorption, previously assigned to the antisymmetric N−H−Br stretching mode,[8] shifts 3.8 cm^{-1} with $^{15}NH_3$ in accord with a small participation for nitrogen in this vibrational mode. The H/D ratio (729.3/480.8 = 1.517) is higher than expected and indicates significant quartic character in the potential function. This is reminiscent of the $(Br-H-Br)^-$ species with a shared proton (728/498 = 1.462).[18] The common frequency position and quartic character in these potential functions are striking and strongly suggest that H_3N−H−Br in solid argon involves a shared proton like that in the $(Br-H-Br)^-$ anion. The 591.3 cm^{-1} band has been assigned to the NH_3 rocking mode,[8] but our calculations place this mode below 300 cm^{-1}; since the N−H−Br bending mode must be reassigned, the 591.3 cm^{-1} band becomes a candidate.

The statistical H, D sample results confirm these assignments: (1) intermediate H, D components at 1079 and 980 cm^{-1} for the 1146.7 cm^{-1} band demonstrate that this is an ammonia submolecule mode; (2) the structure at 729.3, 720.2, 710.8, and 701.3 cm^{-1} shows that mixed H, D is involved in only a secondary manner; hence, this is primarily the antisymmetric N−H−Br stretching mode, and the four subpeaks show that HBr is bonded to ammonia; (3) one broad 595 cm^{-1} absorption again shows that H, D plays a minor role, hence the 591 cm^{-1} band is probably due to the N−H−Br bending mode, although our calculations overestimate this mode. Similar secondary H_3N and D_3N shifts have been observed for the H−F, D−F, and H−Cl stretching modes in the ammonia complexes.[6,10] Accordingly, the single weaker 700.3 and 696.6 cm^{-1} bands in ND_4Br and $^{15}ND_4Br$ experiments can be assigned to the D_3N−HBr stretching modes, as there is a small amount of HBr in the experiments from exchange with the sample tube. Note that the ^{15}N shift on these bands, 3.7 cm^{-1}, is essentially the same as the 3.8 cm^{-1} ^{15}N shift observed for the 729.3 cm^{-1} H_3N−H−Br mode. Furthermore, the sharp 700.3−480.8 cm^{-1} doublet in Figure 4c confirms that a single H(D) atom is primarily involved in this stretching vibration.

Comparison of the argon matrix H_3N−HBr and H_3N−HCl fundamentals[6,8,16] in Table 6 shows that the HBr complex is more affected by the solid argon environment than the HCl complex. The symmetric NH_3 mode is blue shifted 172 cm^{-1} in the former but only 96 cm^{-1} in the latter, and the H−Br mode is red shifted to 28% but the H−Cl mode to only 47% of the argon matrix diatomic molecule values. Clearly argon matrix solvation has supported a greater degree of proton transfer from HBr to NH_3 than from HCl to NH_3.

Neon. The neon matrix experiments are comparable to the argon matrix investigation with two important differences: neon interacts and perturbs less than argon but freezes more slowly at 4−5 K and thus traps less efficiently than argon at 8−9 K. The HBr and $(HBr)_2$ absorptions (Figure 2) are of comparable intensity, but recall that the calculated infrared intensity of the dimer is 100× that of the monomer. The strongest band on deposition at 1079.9 cm^{-1} is associated with weaker 1208.8 and 3444.8 cm^{-1} bands (labeled 1:1); annealing sharpens these features (and in more dilute experiments produces a 10% increase), increases precursor dimers relative to monomers, and produces marked proportional growth in sharp absorptions at 1120.4 cm^{-1} (1:2), 1411.6 cm^{-1} and 1732.6 cm^{-1} (not shown), and a 1389.2 cm^{-1} feature (*x*:*y*). Rapid annealing to 13 K removes most of the neon, and markedly reduces the 1:1 bands, but the higher complexes remain strong while new bands that are appropriate for NH_4Br solid[31] appear. The final spectrum in Figure 2g is the solid NH_4Br film remaining on the cold window after the volatile sample has evaporated.

Assignment of the 1120.4 cm^{-1} band to $(NH_3)(HBr)_2$ follows the same rationale as for the 1111.2 cm^{-1} argon matrix band. Likewise, the sharp 1411.5 and 1732.6 cm^{-1} bands are due to the ionic complex giving the 1397.9 and 1731.9 cm^{-1} argon matrix bands. The torsional motion of NH_4^+ in this complex in neon is 13 cm^{-1} less than in argon. The broader 1389.2 cm^{-1} feature is probably due to a higher ionic complex but still not large enough for an observable ν_3 type mode.

The strong 1079.9 cm^{-1} primary product band exhibits a 5.4 cm^{-1} ^{15}N shift, and the ND_3 counterpart at 831.7 cm^{-1} exhibits a 7.3 cm^{-1} ^{15}N shift; these ^{15}N shifts are slightly more than the corresponding ammonia ν_2 values (4.1, 6.4 cm^{-1}). The H/D ratio (1.298) is higher than the ammonia ν_2 ratio in solid neon (1.262). Mixed $^{14}NH_4Br/^{15}NH_4Br$ experiments gave partially resolved doublets for the 1:1 complex bands, but the sharper deuterium counterparts were resolved doublets at 2569.4, 2556.7 cm^{-1} and at 831.7, 824.4 cm^{-1}, which verifies the participation of a single $NH_3(ND_3)$ submolecule in the 1:1 complex. A spectrum using the statistical H, D sample gave strong new intermediate bands at 1018 and 934 cm^{-1} with pure isotopic 1079.9 and 831.7 cm^{-1} counterparts following the $NH_3/NH_2D/NHD_2/ND_3$ precursor intensities. The 1079.9 cm^{-1} band is clearly due to the symmetric NH_3 bending fundamental in the H_3N−HBr complex. The 3444.8 cm^{-1} absorption sustains isotopic shifts (Table 1) for the antisymmetric NH_3 stretching fundamental in the complex; the D counterparts are more intense for this mode. The weaker associated 1208.8 cm^{-1} band is assigned to the H−Br fundamental. This band exhibits a 6.4 cm^{-1} ^{15}N shift and a DBr counterpart at 947.9 cm^{-1} (H/D = 1208.8/947.9 = 1.275). Although the H−X stretching mode is traditionally expected to be the strongest infrared absorption, the symmetric NH_3 mode is stronger than the H−Cl stretch in H_3N−HCl trapped in solid argon, and the heavier halides have lower intensities. Accordingly, the 1208.8 cm^{-1} band is only slightly weaker relative to the 1079.9 cm^{-1} absorption than the respective modes for H_3N−HCl in solid argon.[16] Finally, only the pure isotopic counterparts 1209 and 948 cm^{-1} were observed in the statistical H, D experiment, which supports the H−Br mode assignment.

Following the examples of H_3N−HF and H_3N−HCl, the neon matrix environment produces a red shift in the H−X fundamental, and it is anticipated that this effect will be increased

for H_3N-HBr because HBr has a lower dissociation energy than HCl. This trend is also demonstrated by the argon matrix spectra.

Neon/Argon. Investigations were done to follow evolution of the spectra when a small amount of more strongly interacting argon is added to the neon host. Slightly perturbed neon matrix spectra were observed with 2% and 5% Ar, and annealing blue shifted 1080 and 1388 cm^{-1} bands in the direction of argon counterparts. On the other hand, slightly perturbed argon matrix spectra were observed with only 10% and 20% argon. This clearly shows that the more strongly interacting argon atoms will replace neon in the "solvent" shell around the H_3N-HBr complex. Similar results were found for H_3N-HCl.[16]

Krypton. The krypton matrix bands can be assigned to the same complexes following the argon matrix absorptions. The stronger krypton matrix effect on the H_3N-HBr complex further shifts the absorptions. The symmetric NH_3 mode is blue shifted another 42 cm^{-1} from the argon matrix position and the $^{15}NH_3$ shift reduced from 4.3 to 3.2 cm^{-1} while the H/D ratio decreases from 1.265 to 1.255. The lower region contains three bands at 700.3, 678.7, and 624.5 cm^{-1} with 9.0, 0.4, and 0.2 cm^{-1} ^{15}N shifts. The straightforward assignment is 700.3 cm^{-1} for the antisymmetric N−H−Br stretching mode and 624.5 cm^{-1} for the N−H−Br bending mode. The sharp 678.7 cm^{-1} band must be a different mode from the 700.3 cm^{-1} band because of the ^{15}N shifts. If the H_3N-HBr complex in solid krypton has reduced symmetry, two N−H−Br bending modes would be expected, and this is a possibility.

Nitrogen. The H_3N-HBr complex was first identified in solid nitrogen[7] from infrared bands at 1754, 1390, 1211, and 300 cm^{-1}. The strongest 1390 cm^{-1} band was assigned as the H−Br stretching mode and the 1211 cm^{-1} band to the corresponding bending mode. Later work maintained these assignments and noted the higher H−Br frequency in solid nitrogen than in argon,[8] which is *opposite* to that observed for the corresponding H−Cl complex.[5−8,16,17]

Our nitrogen matrix experiments with more dilute reagents trap only HBr and NH_3 and form very weak 3402 and 1392 cm^{-1} bands during deposition at 5 K (Figure 7). First annealing to 25 K allows diffusion of trapped reagents and produces the structured 1392.2, 1384.0, 1372.6 cm^{-1} band, a weaker 1211.7 cm^{-1} band, a sharper 3402.7 cm^{-1} absorption (labeled 1:1), and precursor dimer bands. Other features increase markedly on annealing to 36 K, but annealing to 38 K decreases these products in favor of solid-like NH_4Br, which is the only absorber left after 39 K annealing. The sharp 1:2 band at 1127.4 cm^{-1} and bands at 1751.0 and 1429.3 cm^{-1} are assigned to $(NH_3)(HBr)_2$ and a small ionic cluster for the same reasons as the argon and neon matrix analogues. In addition, intermediate mixed H, D components at 1036.8 and 953.4 cm^{-1} for the 1127.4 cm^{-1} band follow the a_1 bending mode of ammonia.

The split 1392.2, 1384.0, 1372.6 cm^{-1} band system reaches maximum intensity on 36 K annealing *before* any observable absorption appears near 3100 cm^{-1} which shows that this feature is not due to solid NH_4Br, in agreement with Ault et al.,[7] but the isotopic data reported here suggest that this band is due to a mixed N−H stretching, NH_3 bending mode and not an H−Br stretching mode as first assigned.[7] First, the structured 1392.2, 1384.0, 1372.6 cm^{-1} band shows 5.2, 4.8, 5.8 cm^{-1} ^{15}N shifts, which are slightly less than that for the ν_4 ammonium ion mode (6.3 cm^{-1}, this work) but larger than the 3.1 cm^{-1} shift for the N−H diatomic oscillator at this frequency. Second, and most important, with statistically mixed H, D ammonium bromide precursor, split strong intermediate bands are observed at 1336.6−1321.9 cm^{-1} and 1134.8−1123.9 cm^{-1}, much like the 1392.2−1372.6 cm^{-1} band but broader than the all-D 1057.8 cm^{-1} counterpart (Figures 7, 8). The new mixed H, D product bands are stronger as are the mixed precursor bands, and the median 62−200−72 cm^{-1} separation is more open in the center than the 65−74−71 cm^{-1} separation for NH_3 $\nu_2(a_1)$. The two mixed H, D counterparts for the 1392.2 cm^{-1} product band clearly demonstrate that this mode involves at least three H, D atoms, but our calculations predict the N−H stretching mode to be 4× stronger than the symmetric NH_3 mode; hence, this absorption is better described as predominantly N−H stretching with mixed symmetric NH_3 bending character. Third, the weaker 1211.7 cm^{-1} band shows mixed H, D counterparts at 1021.5 and probably the sharp weak 1128.2 cm^{-1} peak on top of the 1134.8−1123.9 cm^{-1} feature. These mixed H, D isotopic peaks form a 84−106−78 cm^{-1} separation pattern and suggest the involvement of three H, D atoms in a symmetric NH_3 mode. The mixed H, D isotopic bands rule out the previous N−H−Br bending mode assignment. However, the ^{15}N-shift is smaller than found for ammonia, but in agreement with calculations (1.1 cm^{-1}); this mode is described as mostly symmetric NH_3 bending with mixed N−H stretching character.

Note the intensity reversal of the 1392.2 and 1211.7 cm^{-1} bands on deuteration: the 1057.8 cm^{-1} band is weaker than the 943.6 cm^{-1} band (Figure 8), which suggests a change in the degree of mode mixing on deuterium substitution. The mixed $^{14}ND_4Br/^{15}ND_4Br$ experiment gave 1/1 doublets for the 2536.5, 1057.8, and 943.6 cm^{-1} bands, which verifies the participation of a single ND_3 submolecule in these vibrational modes. The broader 1232 cm^{-1} absorption also appears to be due to the D_3N-DBr complex, and a combination band involving the stronger 943.6 cm^{-1} fundamental and the deuterium counterpart of the low-frequency Br stretching mode is likely. The 3402.7 cm^{-1} band, also reported previously,[8,9] shows the isotopic behavior for a ν_3 type NH_3 mode in the H_3N-HBr complex. Finally, the 1392.2 and 1211.7 cm^{-1} bands are reassigned here to mixed symmetric N−H stretching, NH_3 bending modes of a_1 symmetry in the H_3N-HBr complex, which exhibits more proton transferred in the solid nitrogen host.

There is no stretching frequency involving bromine above the 430 cm^{-1} spectrometer limit; however, the moderately strong 300 cm^{-1} band observed by all three groups[7−9] could be due to the bromine stretching mode, as suggested by Ault et al.[7] Although this assignment has been questioned,[8] the increased ionic character for H_3N-HBr in solid nitrogen might increase this mode above that found for the more covalent H_3N-HCl complex in solid argon.[6] Isotopic shifts will be required to attest this hypothesis.

Bonding Trends. The frequency trends observed for H_3N-HCl and H_3N-HBr complexes in Ne, Ar, Kr, and N_2 matrix hosts are summarized in Table 6. Interaction with the matrix host increases in the above order, and this interaction increases the degree of proton transfer, which is more effective with HBr owing to its lower dissociation energy, and the frequencies vary accordingly. Although microwave spectra of the ground-state complexes ($\upsilon = 0$) argue for little ionic character,[11,13] the halogen nuclear quadrupole coupling constants show that H_3N-HBr is slightly more ionic (18 vs 13%)[17] than H_3N-HCl, and thus the HBr complex is expected to be more vulnerable to matrix effects. In like manner, MP2 calculations show that the $\upsilon = 1$ state of the HBr complex shows more evidence of proton sharing than the $\upsilon = 1$ state of the HCl complex.[20] The H_3N-HBr complex is more ionic and is expected to interact more strongly with all matrix hosts. Thus, the H−Br stretching mode is red shifted to 1208.8 cm^{-1} in solid neon, in solid argon the

mode becomes antisymmetric N−H−Br stretching at 729.3 cm^{-1}, and in solid nitrogen, with more proton transfer, the mode is largely N−H stretching at 1392.2 cm^{-1}. Finally, the corresponding symmetric NH_3 bending mode in H_3N−HBr is blue shifted to 1079.9 cm^{-1} in solid neon and to 1146.7 cm^{-1} in solid argon, much more than their H_3N−HCl counterparts.

Calculations. The DFT calculations presented in Table 5 provide useful frequency predictions. We believe that the B3LYP functional more closely approximates the gas-phase complex because the calculated N−H−Br distance (3.251 Å) is nearly the same as the gas-phase value (3.255 Å).[11] The strong B3LYP harmonic H−Br stretching frequency (1816 cm^{-1}) is probably a good upper-limit approximation of the yet-to-be observed gas phase value. The calculated 6.0 D dipole moment can be represented by a transfer of 0.32 e from N to Br in the absence of polarization. Recent MP2 calculations find nearly the same bond length (3.247 Å) and a slightly higher harmonic frequency (2006 cm^{-1}).[20] The one-dimensional anharmonic correction brings this mode down to 1533 cm^{-1}, which is a reasonable lower-limit for the gaseous complex, but the two-dimensional anharmonic correction to 888 cm^{-1} is clearly excessive, as this is even below our 1209 cm^{-1} neon matrix value, which must be lower than the gas-phase complex. Similarly the two-dimensional correction for H_3N−HCl is excessive (1869 cm^{-1}) as it is also below our neon matrix value (2084 cm^{-1}).[16] We note that the harmonic frequency (716 cm^{-1}) predicted for the H_3N−HBr:3Ar model complex[20] is in excellent agreement with the observed 729 cm^{-1} value, but the same calculation for the 3Ne complex predicts a similar 703 cm^{-1} frequency, which is way out of line with the present experimental observation. However, the addition of an external electric field "tunes" the proton stretching frequency through reasonable values that approximate the matrix observations.[21]

The heptane solvent SCI−PCM calculation[32] produces a much shorter N−H bond length and a larger dipole moment consistent with more proton transfer. The 9.9 D dipole moment is represented by the transfer of 0.68 e from N to Br. The computed frequencies are reasonable although degeneracy is lifted; the strongest calculated infrared intensities are the N−H stretching mode at 1460 cm^{-1}, the symmetric NH_3 bending mode at 1256 cm^{-1}, and the H_3NH−Br stretching mode at 328 cm^{-1}. These calculated frequencies match the nitrogen matrix spectrum amazingly well and certainly support the conclusion that the nitrogen matrix solvates the polar H_3N−HBr complex, increases the degree of proton transfer, and affects the vibrational spectrum accordingly.

Conclusions

Ammonia and hydrogen bromide vapors from the thermal decomposition of NH_4Br were co-deposited with excess neon at 4−5 K to form the H_3N−HBr complex. New 3444.8, 1208.8, and 1079.9 cm^{-1} infrared absorptions are assigned to the antisymmetric NH_3 stretching, H−Br stretching, and symmetric NH_3 bending modes of the 1:1 complex. Vibrational assignments are supported by $^{15}NH_4Br$, ND_4Br, $^{15}ND_4Br$, and mixed H, D isotopic substitution. Complementary experiments were done with neon/argon mixtures, argon, krypton, and nitrogen to investigate the 1:1 complex in a range of matrix environments. The above modes are shifted to 3420.8, 729.3, and 1146.7 cm^{-1} in solid argon owing to an increased interaction with the matrix and the resulting increased proton sharing. The neon matrix spectrum suggests a strong hydrogen bond, slightly stronger than in the gas-phase complex but not as strong as found in the argon and krypton matrix hosts owing to increased solvation by the more polarizable matrix atoms and more proton transfer.

The H_3N−HBr complex is produced in dilute reagent solid nitrogen experiments on annealing to allow diffusion and association of reagent molecules. The strong nitrogen matrix infrared absorption at 1392.2 cm^{-1}, which shows a 5.2 cm^{-1} ^{15}N shift, 1336.6 and 1134.8 cm^{-1} mixed H, D and 1058.0 cm^{-1} ND_4Br counterparts, is due to a mixed N−H stretching, NH_3 bending mode: this suggests even more proton transfer in the nitrogen matrix host. These and earlier[7−9] matrix isolation experiments demonstrate that the matrix environment markedly affects the hydrogen bonding interaction and the degree of proton transfer in the polar H_3N−HBr complex.

On annealing solid matrix samples containing HBr and NH_3, the H_3N−HBr complex and higher clusters are formed, which ultimately lead to solid NH_4Br (Figures 2 and 7). A small ionic complex was produced in all four matrices and characterized by solid-like ν_4 fundamental and $\nu_4+\nu_6$ combination bands. The NH_4^+ torsional frequency (ν_6) in this matrix-isolated ionic complex is essentially the same as in solid NH_4Br, which supports proton transfer and the ionic model for small complexes.

Finally, DFT calculations are useful to predict the complex frequencies and to model the effect of matrix solvation.

Acknowledgment. We acknowledge the assistance of Z. Mielke and B. Liang with preliminary experiments, helpful correspondence with C. W. Bauschlicher, Jr., and financial support from N. S. F. Grant CHE 00-78836.

References and Notes

(1) Clementi, E. *J. Chem. Phys.* **1967**, *46*, 3851; *47*, 2323.
(2) Raffenetti, R. C.; Phillips, D. H. *J. Chem. Phys.* **1979**, *71*, 4534.
(3) Latajka, Z.; Scheiner, S. *J. Chem. Phys.* **1984**, *81*, 4014. Latajka, Z.; Scheiner, S.; Ratajczak, H. *Chem. Phys Lett.* **1987**, *135*, 367.
(4) Brciz, A.; Karpfen, A.; Lischka, H.; Schuster, P. *Chem. Phys.* **1984**, *89*, 337.
(5) Ault, B. S.; Pimentel, G. C. *J. Phys. Chem.* **1973**, *77*, 1649.
(6) Barnes, A. J.; Beech, T. J.; Mielke, Z. *J. Chem. Soc., Faraday Trans. 2* **1984**, *80*, 455.
(7) Ault, B. S.; Steinbach, E.; Pimentel, G. C. *J. Phys. Chem.* **1975**, *79*, 615.
(8) Barnes, A. J.; Wright, M. P. *J. Chem. Soc., Faraday Trans. 2* **1986**, *82*, 153.
(9) Schriver, L.; Schriver, A.; Perchard, J. P. *J. Am. Chem. Soc.* **1983**, *105*, 3843.
(10) Johnson, G. L.; Andrews, L. *J. Am. Chem. Soc.* **1982**, *104*, 3043.
(11) Howard, N. W.; Legon, A. C. *J. Chem. Phys.* **1987**, 86, 6722.
(12) Howard, N. W.; Legon, A. C. *J. Chem. Phys.* **1988**, *88*, 4694.
(13) Legon, A. C. *Chem. Soc. Rev.* **1993**, 153 and references therein.
(14) Andrews, L. In *Chemistry and Physics of Matrix Isolated Species*; Andrews, L., Moskovits, M., Eds.; Elsevier: Amsterdam, 1989; Chapter 2.
(15) Thomas, R. K., unpublished 3215 cm^{-1} absorption for H−F mode in H_3N−HF complex, personal communication, 1981. Miller, R. E., unpublished 3230 cm^{-1} fundamental, personal communication, 2001. See Miller, R. E. *Science* **1988**, *240*, 447.
(16) Andrews, L.; Wang, X.; Mielke, Z. *J. Am. Chem. Soc.* **2001**, *123*, 1499; *J. Phys. Chem. A* **2001**, in press.
(17) Barnes, A. J.; Legon, A. C. *J. Mol. Struct.* **1998**, *448*, 101.
(18) Milligan, D. E.; Jacox, M. E. *J. Chem. Phys.* **1971**, *55*, 2550.
(19) Del Bene, J. E.; Jordan, M. J. T.; Gill, P. M. W.; Buckingham, A. D. *Mol. Phys.* **1997**, *92*, 429.
(20) Del Bene, J. E.; Jordan, M. J. T. *J. Chem. Phys.* **1998**, *108*, 3205.
(21) Jordan, M. J. T.; Del Bene, J. E. *J. Am. Chem. Soc.* **2000**, *122*, 2101.
(22) Temperature measured by chromal−alumel thermocouple placed between heater tape and sample tube. Vapor pressure 2 to 18 mTorr, *Handbook of Chemistry and Physics*, D-139, Chemical Rubber Publishing Co., Cleveland, Ohio, 1968. The ND_4Br sample prepared here appears to be more volatile than the commercial NH_4Br sample as approximately 10 °C lower evaporation temperature was employed for comparable ND_4Br experiments. Furthermore, a mixture of NH_4Br and ND_4Br gave 10× stronger ND_3 absorption than NH_3, and the first experiment with the statistical H, D mixture gave a 43/131/120/38 mau isotopic quartet, but subsequent experiments were steadily depleted in the more deuterated isotopic species.

(23) Suzer, S.; Andrews, L. *J. Chem. Phys.* **1987**, *87*, 5131.

(24) Frisch, M. J.; Trucks, G. W.; Schlegel, H. B.; Scuseria, G. E.; Robb, M. A.; Cheeseman, J. R.; Zakrzewski, V. G.; Montgomery, J. A., Jr.; Stratmann, R. E.; Burant, J. C.; Dapprich, S.; Millam, J. M.; Daniels, A. D.; Kudin, K. N.; Strain, M. C.; Farkas, O.; Tomasi, J.; Barone, V.; Cossi, M.; Cammi, R.; Mennucci, B.; Pomelli, C.; Adamo, C.; Clifford, S.; Ochterski, J.; Petersson, G. A.; Ayala, P. Y.; Cui, Q.; Morokuma, K.; Malick, D. K.; Rabuck, A. D.; Raghavachari, K.; Foresman, J. B.; Cioslowski, J.; Ortiz, J. V.; Stefanov, B. B.; Liu, G.; Liashenko, A.; Piskorz, P.; Komaromi, I.; Gomperts, R.; Martin, R. L.; Fox, D. J.; Keith, T.; Al-Laham, M. A.; Peng, C. Y.; Nanayakkara, A.; Gonzalez, C.; Challacombe, M.; Gill, P. M. W.; Johnson, B. G.; Chen, W.; Wong, M. W.; Andres, J. L.; Head-Gordon, M.; Replogle, E. S.; Pople, J. A. *Gaussian 98*, revision x.x; Gaussian, Inc.: Pittsburgh, PA, 1998.

(25) (a) Becke, A. D. *Phys. Rev. A* **1988**, *38*, 3098. (b) Perdew, J. P.; Wang, Y. *Phys. Rev. B* **1992**, *45*, 13244.

(26) (a) Becke, A. D. *J. Chem. Phys.* **1993**, *98*, 5648. (b) Lee, C.; Yang, W.; Parr, R. G. *Phys. Rev. B* **1988**, *37*, 785.

(27) (a) Krishnan, R.; Binkley, J. S.; Seeger, R.; Pople, J. A. *J. Chem. Phys.* **1980**, *72*, 650. (b) Frisch, M. J.; Pople, J. A.; Binkley, J. S. *J. Chem. Phys.* **1984**, *80*, 3265.

(28) Hay, P. J.; Wadt, W. R. *J. Chem. Phys.* **1985**, *82*, 270. Wadt, W. R.; Hay, P. J. *J. Chem. Phys.* **1985**, *82*, 284. Hay, P. J.; Wadt, W. R. *J. Chem. Phys.* **1985**, *82*, 299.

(29) Abouaf-Marguin, L.; Jacox, M. E.; Milligan, D. E. *J. Mol. Spectrosc.* **1977**, *67*, 34.

(30) Girardet, C.; Maillard, D.; Schriver, A.; Perchard, J. P. *J. Chem. Phys.* **1979**, *70*, 1511. Maillard, D.; Schriver, A.; Perchard, J. P.; Girardet, C. *J. Chem. Phys.* **1979**, *71*, 505.

(31) Wagner, E. L.; Hornig, D. F. *J. Chem. Phys.* **1950**, *18*, 305.

(32) Foresman, J. B.; Keith, T. A.; Wiberg, K. B.; Snoonian, J.; Frisch, M. J. *J. Phys. Chem.* **1996**, *100*, 16098.

(33) Huber, K. P.; Herzberg, G. *Constants of Diatomic Molecules*; Van Nostrand Reinhold: New York, 1979.

(34) Tao, F.-M. *J. Chem. Phys.* **1999**, *110*, 11121.